Endoplasmic reticulum stress leads to accumulation of wild-type SOD1 aggregates associated with sporadic amyotrophic lateral sclerosis

Danilo B. Medinas[a,b,c,1], Pablo Rozas[a,b,c], Francisca Martínez Traub[a,b,c], Ute Woehlbier[a,c,d], Robert H. Brown[e], Daryl A. Bosco[e], and Claudio Hetz[a,b,c,f,g,1]

[a]Biomedical Neuroscience Institute, Faculty of Medicine, University of Chile, Santiago, Chile 8380453; [b]Center for Geroscience, Brain Health and Metabolism, Santiago, Chile 7800003; [c]Program of Cellular and Molecular Biology, Institute of Biomedical Sciences, University of Chile, Santiago, Chile 8380453; [d]Center for Integrative Biology, Faculty of Science, Universidad Mayor, Santiago, Chile 8580745; [e]Department of Neurology, University of Massachusetts Medical School, Worcester, MA 01605; [f]Buck Institute for Research on Aging, Novato, CA 94945; and [g]Department of Immunology and Infectious Diseases, Harvard School of Public Health, Boston, MA 02115

Edited by Gregory A. Petsko, Weill Cornell Medical College, New York, NY, and approved June 28, 2018 (received for review January 20, 2018)

Abnormal modifications to mutant superoxide dismutase 1 (SOD1) are linked to familial amyotrophic lateral sclerosis (fALS). Misfolding of wild-type SOD1 ($SOD1^{WT}$) is also observed in postmortem tissue of a subset of sporadic ALS (sALS) cases, but cellular and molecular mechanisms generating abnormal $SOD1^{WT}$ species are unknown. We analyzed aberrant human $SOD1^{WT}$ species over the lifetime of transgenic mice and found the accumulation of disulfide–cross-linked high–molecular-weight $SOD1^{WT}$ aggregates during aging. Subcellular fractionation of spinal cord tissue and protein overexpression in NSC-34 motoneuron-like cells revealed that endoplasmic reticulum (ER) localization favors oxidation and disulfide-dependent aggregation of $SOD1^{WT}$. We established a pharmacological paradigm of chronic ER stress in vivo, which recapitulated $SOD1^{WT}$aggregation in young transgenic mice. These species were soluble in nondenaturing detergents and did not react with a SOD1 conformation-specific antibody. Interestingly, $SOD1^{WT}$ aggregation under ER stress correlated with astrocyte activation in the spinal cord of transgenic mice. Finally, the disulfide–cross-linked $SOD1^{WT}$ species were also found augmented in spinal cord tissue of sALS patients, correlating with the presence of ER stress markers. Overall, this study suggests that ER stress increases the susceptibility of $SOD1^{WT}$ to aggregate during aging, operating as a possible risk factor for developing ALS.

amyotrophic lateral sclerosis | wild-type SOD1 | ER stress | aging | protein aggregation

Amyotrophic lateral sclerosis (ALS) is characterized by selective degeneration of motoneurons from cerebral cortex, brainstem, and spinal cord leading to muscle weakness, atrophy, paralysis, and premature death (1, 2). Most ALS cases are considered sporadic (sALS), while 10% are familial (fALS), involving mutations in superoxide dismutase 1 (SOD1), transactive response DNA binding protein 43 (TARDBP or TDP-43), fused in sarcoma/translocated in sarcoma (FUS/TLS), and the hexanucleotide repeat expansions in C9ORF72 as the most common alterations (1–3).

More than 150 mutations in SOD1 have been linked to ALS, with varying degrees of aggressiveness and aggregation propensity (4). SOD1 folding depends on complex posttranslational modifications, including the insertion of zinc and copper ions and intramolecular disulfide-bond formation, followed by homodimerization (4). Biochemical studies have shown that fALS-linked mutations destabilize SOD1 polypeptide, preventing its posttranslational processing with resultant accumulation of aggregation-prone species (5). Mutant SOD1 toxicity may be the result of disturbed cellular homeostasis at many levels, such as axonal transport, the cytoskeleton, mitochondrial function, and the secretory pathway, in addition to cell-nonautonomous mechanisms marked by the abnormal activation of microglia and astrocytes (6, 7).

Several studies have reported the presence of abnormal $SOD1^{WT}$ species in postmortem sALS tissue using conformation-specific antibodies that recognize misfolded forms of the protein, possibly corresponding to small and diffusible oligomeric species that do not accumulate into high–molecular-weight (HMW) aggregates (8–10). Misfolded $SOD1^{WT}$ can exhibit toxic properties by impairing axonal transport, inhibiting endoplasmic reticulum (ER)-associated degradation, and self-propagating its misfolding in a prion-like fashion (9–12). At the molecular level, altered posttranslational maturation of $SOD1^{WT}$ can trigger its misfolding and aggregation (9, 13, 14). Interestingly, coexpression of human $SOD1^{WT}$ together with fALS-linked SOD1 mutants aggravates disease severity in ALS mouse models, and homozygous $SOD1^{WT}$ transgenic mice develop late-onset motor disease (15, 16). Despite representing an attractive hypothesis of convergent disease mechanisms of sALS and fALS, the overall relevance of $SOD1^{WT}$ to sALS has been questioned because of low frequency or lack of staining with conformation-specific antibodies in some studies (17, 18).

Altered proteostasis is a common pathogenic hallmark of both sALS and many different forms of fALS (19). One of the main nodes of the proteostasis network affected in ALS is the ER (20), the major subcellular compartment involved in protein folding and quality control mechanisms. ER stress triggers an adaptive reaction known as the unfolded protein response (UPR) to restore

Significance

The identification of aberrant $SOD1^{WT}$ species accumulating in the spinal cord during aging could reveal pathogenic species involved in sporadic (s)ALS. Using a combination of biochemical approaches, we discovered that disulfide–cross-linked $SOD1^{WT}$ aggregates rise before other abnormal protein species during aging and are significantly increased in sALS spinal cord tissue. We also found that endoplasmic reticulum stress stimulates accumulation of these species, with involvement of tryptophan-32 oxidation. These results establish a connection between $SOD1^{WT}$ aggregation and a major proteostasis network affected in ALS.

Author contributions: D.B.M., U.W., R.H.B., D.A.B., and C.H. designed research; D.B.M., P.R., and F.M.T. performed research; D.A.B. contributed new reagents/analytic tools; R.H.B. provided human tissue; D.B.M., P.R., and F.M.T. analyzed data; and D.B.M. and C.H. wrote the paper.

The authors declare no conflict of interest.

This article is a PNAS Direct Submission.

Data deposition: Raw data available at www.hetzlab.cl/data/.

[1]To whom correspondence may be addressed. Email: dmedinas@med.uchile.cl or chetz@med.uchile.cl.

This article contains supporting information online at www.pnas.org/lookup/suppl/doi:10.1073/pnas.1801109115/-/DCSupplemental.

Published online July 23, 2018.

proteostasis by attenuating protein translation and reprogramming gene expression to up-regulate ER foldases, chaperones, and the protein degradation machinery (21). However, high levels of chronic ER stress result in apoptosis (22). In the context of mutant SOD1, ER stress is proposed as a key factor determining selective neuronal vulnerability (23). Strategies to attenuate ER stress levels have been shown to delay experimental ALS (24). SOD1 is predominantly cytosolic, and although it does not have an ER-localization signal peptide, a small fraction of the protein is released to the extracellular space through the classical secretory pathway (25, 26). Here we investigated the relationship between ER stress, $SOD1^{WT}$ misfolding, and aging. Our results support a pathogenic role of ER stress in sALS by inducing abnormal $SOD1^{WT}$ aggregation at the ER during aging.

Results

Disulfide–Cross-Linked $SOD1^{WT}$ Aggregates Accumulate During Aging. The buffering capacity of the proteostasis network decreases during aging (27); we reasoned that this may increase the accumulation of misfolded SOD1 species. We performed analysis of $SOD1^{WT}$ aggregates with different approaches in young (4-mo), middle-aged (8-mo), and old (16-mo) heterozygous human $SOD1^{WT}$ transgenic mice (see schema in *SI Appendix*, Fig. S1*A*). As a positive control for the methods, we analyzed $SOD1^{G93A}$ transgenic mice (*SI Appendix*, Fig. S1 *B–D*). Using the filter-trap assay, we observed a progressive accumulation of HMW $SOD1^{WT}$ aggregates, starting at 4 mo of age, with further increase in older mice (Fig. 1*A*). We also assessed the possible involvement of disulfide bonds in human $SOD1^{WT}$ protein aggregation by treating samples with the thiol-reducing agent DTT. Disulfide-independent $SOD1^{WT}$ aggregates were barely detectable in younger mice, with strong accumulation at 16 mo of age only (Fig. 1*A*).

We then monitored detergent-insoluble $SOD1^{WT}$ aggregates by centrifugal sedimentation (*SI Appendix*, Fig. S1*C*), which only showed a significant increase in aged mice (Fig. 1*B*). Since $SOD1^{WT}$ oxidation had been implicated in sALS and may contribute to its misfolding (13, 28), we measured protein carbonylation in $SOD1^{WT}$ transgenic mice. The identification of carbonylated $SOD1^{WT}$ could be easily inferred by comparison of band pattern in transgenic mice and nontransgenic littermates (Fig. 1*C*). Carbonylated $SOD1^{WT}$ was significantly accumulated in older animals, whereas the overall pattern of protein oxidation did not change across ages (Fig. 1*C*).

Next, we focused on detecting misfolded soluble $SOD1^{WT}$ species using conformation-specific antibodies that were generated using the $SOD1^{G93A}$ antigen but recognize modified $SOD1^{WT}$ species (9, 29). The monoclonal antibody B8H10 was employed since it yielded satisfactory immunoprecipitation of SOD1 (*SI Appendix*, Fig. S1*D*). We consistently detected B8H10-positive $SOD1^{WT}$ in transgenic mice at the three ages analyzed, with variable amounts between animals (Fig. 1*D*). Contrary to the trend observed for other species, B8H10-positive $SOD1^{WT}$ was reduced with aging (Fig. 1*D*). Overall, disulfide-dependent $SOD1^{WT}$ aggregates accumulate earlier in the aging process relative to other $SOD1^{WT}$ species (see summary in Fig. 1*E*).

Accumulation of HMW $SOD1^{WT}$ Aggregates in Microsomal Fractions During Aging. To define the distribution of disulfide–cross-linked $SOD1^{WT}$ species during aging, we performed subcellular fractionation of spinal cord tissue of animals at different ages using differential

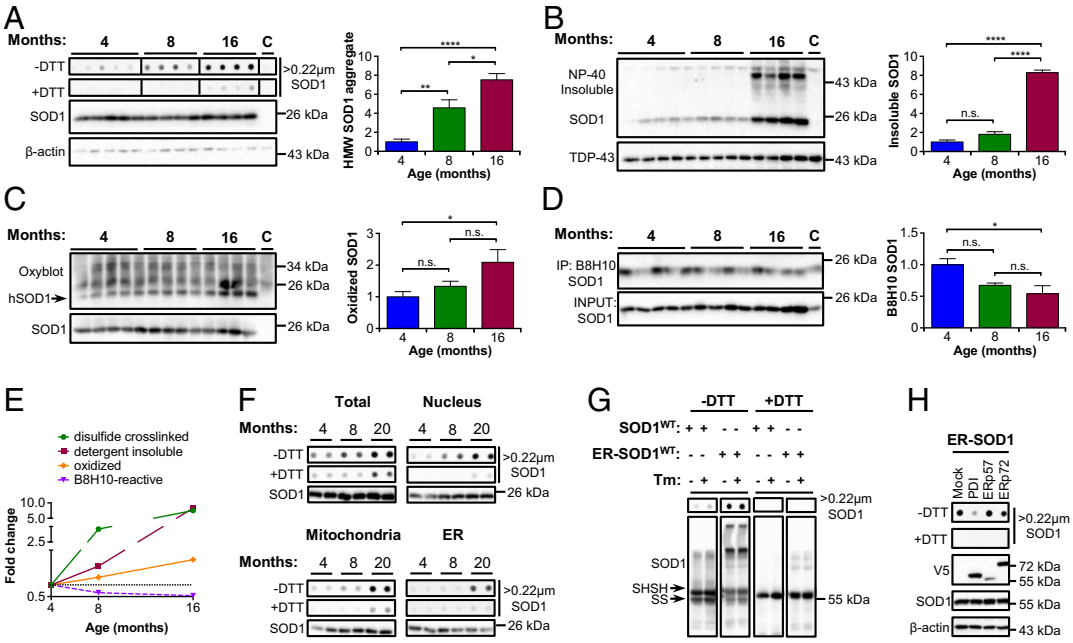

Fig. 1. Misfolding and aggregation of $SOD1^{WT}$ during aging. The spinal cord of $SOD1^{WT}$-Tg mice was analyzed at the indicated ages. (*A*) Filter-trap assay under nonreducing (–DTT) and reducing (+DTT) conditions. β-Actin was employed as loading control. (*B*) Western blot analysis of nonionic detergent (Nonidet P-40)-insoluble SOD1 aggregates isolated by centrifugal sedimentation. TDP-43 was used as loading control. (*C*) Western blot analysis of carbonylated (oxidized) proteins. SOD1 was employed as loading control. The arrow indicates oxidized $SOD1^{WT}$. (*D*) Western blot analysis of SOD1 immunoprecipitation (IP) with B8H10 conformation-specific antibody. SOD1 in the input was used as loading control. A 16-mo-old non-Tg littermate was used in *A–C* as control for background (lane labeled "C"). A symptomatic $SOD1^{G93A}$-Tg mouse was used in *D* as positive control (lane labeled C). Statistical analysis (*A–D*) was performed using one-way ANOVA with Tukey's multiple comparison test. Mean ± SE is shown; *P* values are as follows: n.s., not significant, $P > 0.05$; $*P \leq 0.05$; $**P \leq 0.01$; $****P \leq 0.0001$. $n = 4$ or 5 per group. (*E*) Fold-change plot for accumulation of the distinct abnormal $SOD1^{WT}$ species during aging. (*F*) Filter-trap assay of spinal cord subcellular fractions of $SOD1^{WT}$-Tg mice at different ages. SOD1 was employed as loading control. (*G*) NSC-34 cells were transiently transfected for overexpression of $SOD1^{WT}$-EGFP or ER-$SOD1^{WT}$-EGFP and treated with tunicamycin (Tm; 1 μg/mL). Filter-trap and Western blot analyses were performed under nonreducing and reducing conditions after 18 h of Tm treatment. Arrows indicate reduced (SHSH) or oxidized (SS) $SOD1^{WT}$ monomer. (*H*) NSC-34 cells were transiently transfected for coexpression of $SOD1^{WT}$-EGFP or ER-$SOD1^{WT}$-EGFP and the indicated PDI family member. Filter-trap and Western blot analyses were performed 48 h after transfection.

centrifugation. Filter-trap analysis of total extracts confirmed our previous finding indicating that disulfide-dependent SOD1^{WT} aggregates accumulate progressively during the lifetime, while disulfide-independent species are increased in aged animals (Fig. 1*F*). Nucleus- and mitochondria-enriched fractions contained most of the SOD1^{WT} aggregates, with disulfide-dependent and -independent aggregates increasing with aging (Fig. 1*F*). On the other hand, microsomal (ER-enriched) fractions predominantly accumulated disulfide–cross-linked SOD1^{WT} aggregates in older mice, with negligible levels of DTT-insensitive species (Fig. 1*F*). This result indicates that disulfide-dependent SOD1^{WT} aggregation is favored at the ER.

We investigated whether directing expression of human SOD1^{WT} to the ER lumen influences protein aggregation. Thus, we transiently expressed in NSC-34 cells a previously described SOD1^{WT} fused to EGFP that is targeted to the ER lumen (ER-SOD1^{WT}) (*SI Appendix*, Fig. S2*A*) (26). Remarkably, expression of ER-SOD1^{WT} led to a dramatic accumulation of HMW aggregates that were sensitive to DTT treatment as detected using filter-trap and Western blot analysis (Fig. 1*G*). The stimulation of ER stress with tunicamycin (Tm) in vitro triggered a slight increase in these species (Fig. 1*G*). Disulfide bonds at the ER are catalyzed by a family of protein disulfide isomerase (PDI) (30). We tested the effects of coexpressing major PDIs with ER-SOD1^{WT}. The overexpression of PDI or ERp72 significantly reduced the disulfide-dependent HMW aggregates (Fig. 1*H* and *SI Appendix*, Fig. S2*B*), indicating that altered redox folding drives SOD1^{WT} aggregation in the ER. Taken together, these results suggest that ER localization of SOD1^{WT} favors protein aggregation in a specific manner.

ER Stress Leads to Disulfide-Dependent Aggregation of SOD1^{WT}. ER stress is a salient feature of sALS, and has been proposed as a major pathological reaction in various experimental models of the disease (20). We first monitored expression levels of the ER stress-inducible genes *Xbp1s*, *Bip*, and *Edem1* in the spinal cord of SOD1^{WT} transgenic mice and littermate controls and observed a significant increase in both groups at 16 mo of age (Fig. 2*A* and *SI Appendix*, Fig. S3*A*). The induction of *Edem1* levels with aging was even higher in SOD1^{WT} transgenic mice, possibly reflecting disturbed ER function (Fig. 2*A*). We then investigated whether ER stress could trigger SOD1^{WT} misfolding and aggregation using a pharmacological paradigm based on the injection of tunicamycin leading to activation of the UPR in the nervous system (Fig. 2 *B* and *C* and *SI Appendix*, *Results* and Fig. S3 *B*–*F*).

We compared the possible effects of chronic and acute ER stress on SOD1^{WT} aggregation. Filter-trap analysis revealed that mice exposed to chronic ER stress presented accumulation of disulfide–cross-linked SOD1^{WT} aggregates in spinal cord tissue at 4 mo of age (Fig. 2*D*). This effect was not observed in animals treated with an acute regimen of tunicamycin (Fig. 2*D*). Unexpectedly, neither detergent-insoluble species nor B8H10-positive SOD1^{WT} showed significant changes under chronic or acute ER stress (*SI Appendix*, Fig. S3 *G* and *H*). Chronic ER stress also further increased the accumulation of disulfide-dependent SOD1^{WT}

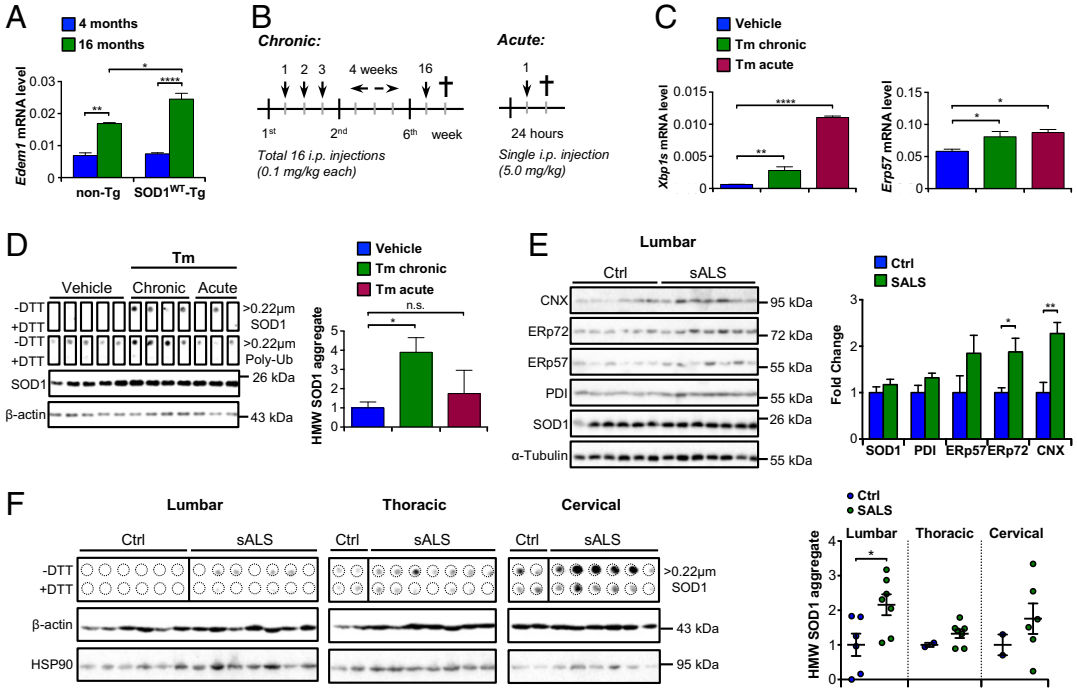

Fig. 2. Disulfide–cross-linked SOD1^{WT} aggregates in transgenic mice under ER stress and in sALS patients. (*A*) mRNA levels of the ER stress marker *Edem1* were analyzed by quantitative PCR in the spinal cord of SOD1^{WT}-Tg mice and non-Tg littermates at different ages ($n = 3$ to 6 per group). (*B*) Schematic view of the protocol for induction of chronic and acute ER stress in vivo. In the chronic paradigm, mice were treated with a total of 16 low doses of tunicamycin (Tm). In the acute protocol, mice received a single high-dose injection of Tm. (*C*) mRNA levels of the ER stress markers *Xbp1s* and *Erp57* were analyzed by quantitative PCR in the spinal cord of SOD1^{WT}-Tg mice submitted to Tm treatments. (*D*) Filter-trap assay of total spinal cord extracts of hSOD1^{WT}-Tg mice described in *C* under nonreducing (−DTT) and reducing (+DTT) conditions for detection of HMW SOD1 and polyubiquitinated aggregates. Duplicated membranes were employed in this analysis. β-Actin was employed as loading control. Statistical analysis was performed using two-way ANOVA (*A*) or one-way ANOVA (*C* and *D*) with Tukey's multiple comparison test. Mean ± SE is shown; *P* values are as follows: n.s., $P > 0.05$; *$P \le 0.05$; **$P \le 0.01$; ****$P \le 0.0001$. $n = 3$ to 6 per group. Frozen postmortem spinal cord tissue of sALS patients and controls (*SI Appendix*, Table S1) was processed for biochemical analysis. (*E*) Western blot analysis of SOD1 and ER chaperone levels in lumbar spinal cord of sALS cases and controls. α-Tubulin was employed as loading control. CNX, calnexin. (*F*) Filter-trap assay of total spinal cord extracts of sALS cases and controls under nonreducing (−DTT) and reducing (+DTT) conditions for detection of HMW SOD1 aggregates. β-Actin was employed as loading control. (*Left*) Lumbar, (*Middle*) thoracic, and (*Right*) cervical spinal cord segments. Statistical analysis was performed using Student's *t* test. Mean ± SE is shown; *P* values are as follows: n.s., $P > 0.05$; *$P \le 0.05$; **$P \le 0.01$. $n = 6$ or 7 per group.

aggregates in animals at 16 mo of age (*SI Appendix*, Fig. S4). Furthermore, the treatment of the NSC-34 cells with tunicamycin induced aggregation of endogenous SOD1 (*SI Appendix*, Fig. S5), reinforcing the significance of our findings in the transgenic model. Thus, our pharmacological paradigm for chronic ER stress in vivo was able to accelerate the appearance of a biochemical fingerprint of $SOD1^{WT}$ aggregation that spontaneously occurs during aging.

Increased Levels of Disulfide–Cross-Linked $SOD1^{WT}$ Aggregates in sALS Tissue. We then addressed the possible association of disulfide–cross-linked $SOD1^{WT}$ aggregates with sALS by investigating postmortem samples. We analyzed lumbar spinal cord tissue of six control subjects and seven sALS patients, in addition to two control and seven sALS samples of thoracic and two control and six sALS samples of cervical segments as available (see the clinical and histopathological data of patients in *SI Appendix*, Table S1). We confirmed the occurrence of ER stress in human sALS tissue, reflected in significant up-regulation of calnexin and ERp72, using Western blot (Fig. 2*E*). Total SOD1 levels were not altered. We performed filter-trap assay to assess the possible accumulation of $SOD1^{WT}$ aggregated species. Remarkably, disulfide-dependent HMW $SOD1^{WT}$ aggregates were significantly augmented in the lumbar spinal cord of patients (4 positive/7 total) compared with control (0 positive/6 total) subjects (Fig. 2*F*). In addition, a trend to an increase of these $SOD1^{WT}$ species was also observed in thoracic (5 positive/7 total) and cervical (3 positive/6 total) segments of the spinal cord of sALS cases, with no relevant accumulation found in the two control samples for each region (Fig. 2*F*). These results suggest that HMW aggregates of $SOD1^{WT}$ are present in sALS spinal cord tissue and correlate with the up-regulation of ER stress-responsive chaperones.

Selective Activation of Astrocytes in $SOD1^{WT}$ Transgenic Mice Under ER Stress. To explore the possible occurrence of pathological changes induced by chronic ER stress in the context of human $SOD1^{WT}$ overexpression, we investigated lumbar spinal cord alterations using histological methods. We performed immunohistochemical analysis with choline acetyltransferase (ChAT) antibody to quantify motoneuron number. This analysis did not reveal any evident neuronal loss in mice submitted to ER stress (Fig. 3*A*). We then evaluated glial responses by monitoring the activation of microglia and astrocytes using immunofluorescence. Remarkably, we observed selective and marked activation of astrocytes in the spinal cord ventral horn of $SOD1^{WT}$ transgenic mice under ER stress (Fig. 3*B*). Nontransgenic animals did not show any activation of astrocytes under the same conditions (Fig. 3*B*). In contrast, ER stress did not induce the differential activation of microglia in any experimental group (Fig. 3*C*). These results suggest a correlation between $SOD1^{WT}$ aggregation and abnormal astrocyte activation under ER stress.

Tryptophan-32 Oxidation Enhances $SOD1^{WT}$ Aggregation at the ER. To gain insights about the molecular alterations that could contribute to $SOD1^{WT}$ aggregation during ER stress, we first measured protein carbonylation of $SOD1^{WT}$ since it can trigger its misfolding and aggregation in vitro (9, 13). Nonetheless, both chronic and acute ER stress caused an increment of carbonylated $SOD1^{WT}$ (Fig. 4*A*). Total levels of carbonylation did not change with overexpression of human $SOD1^{WT}$ (Fig. 4*A*).

Next, we focused on identifying specific $SOD1^{WT}$ posttranslational modifications that could potentially impart aggregation-prone motifs to the protein. We purified $SOD1^{WT}$ using immunoprecipitation of subcellular fractions of spinal cord tissue under basal and chronic ER stress conditions, followed by enzymatic digestion and mass spectrometry analysis. Screening for modifications in key residues previously known to be involved in $SOD1^{WT}$ misfolding and aggregation (31) revealed higher levels of oxidized tryptophan 32 (W32) in

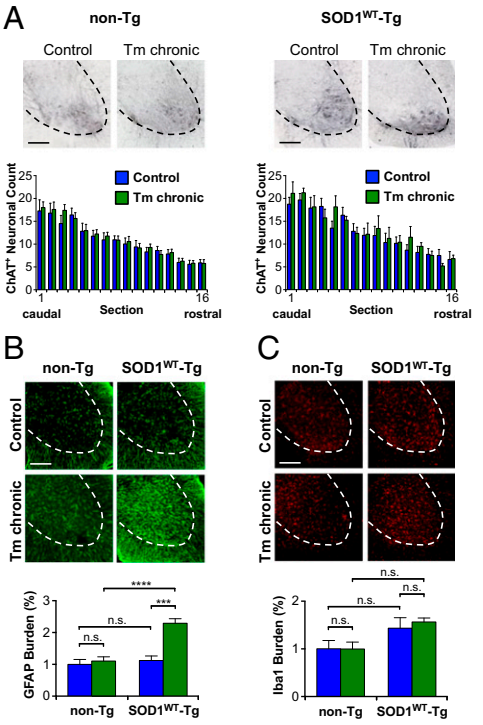

Fig. 3. Histopathological alterations in $SOD1^{WT}$ transgenic mice exposed to ER stress. $SOD1^{WT}$-Tg mice and non-Tg littermates were submitted to chronic tunicamycin or vehicle treatment and histopathological analysis was performed in lumbar spinal cord. (*A*) Representative images of ChAT staining for visualization of motoneurons in the spinal cord ventral horn. Graphs show quantification of motoneuron number in 200-μm-spaced serial sections spanning from L2 to L5 lumbar spinal cord. (*B*) Representative images of GFAP staining for detection of astrocytes. Graphs show the relative mean of gray matter area covered by astrocytes as quantified in four 800-μm-spaced serial sections spanning from L2 to L5 lumbar spinal cord. (*C*) Representative images of Iba1 staining for detection of microglia. Graphs show the relative mean of gray matter area covered by microglia as quantified in four 800-μm-spaced serial sections spanning from L2 to L5 lumbar spinal cord. (Scale bars, 200 μm.) Statistical analysis was performed using two-way ANOVA with Tukey's multiple comparison test. Mean ± SE is shown; *P* values are as follows: n.s., $P > 0.05$; ***$P \leq 0.001$; ****$P \leq 0.0001$. $n = 6$ to 11 per group.

$SOD1^{WT}$ purified from microsomal fractions (Fig. 4 *B* and *C* and *SI Appendix*, Fig. S6). Upon ER stress, increased W32 oxidation was also detected in cytosolic and mitochondrial pools of the protein (Fig. 4 *B* and *C*).

To understand the impact of W32 oxidation on $SOD1^{WT}$ aggregation, we performed site-directed mutagenesis to substitute W32 for phenylalanine (W32F), an amino acid with aromatic properties but resistant to oxidative modifications. Using overexpression of $SOD1^{WT}$ and ER-targeted $SOD1^{WT}$ in NSC-34 cells, we determined that W32F substitution significantly diminishes total protein levels and the formation of HMW disulfide-dependent $SOD1^{WT}$ aggregates in the ER (Fig. 4*D*). These results suggest that the ER environment significantly contributes to abnormal posttranslational modification of $SOD1^{WT}$ and its aggregation.

Discussion

A pathogenic role of $SOD1^{WT}$ has been inferred from the detection of misfolded forms of the protein in postmortem tissue of sALS patients (12). The current evidence supporting $SOD1^{WT}$ misfolding in sALS is mainly based on immunohistochemical staining of paraffin-embedded formalin-fixed spinal cord tissue of patients using conformation-specific antibodies (8–10). This approach is inherently difficult since misfolded SOD1 reactive toward conformation-specific antibodies is mainly constituted by

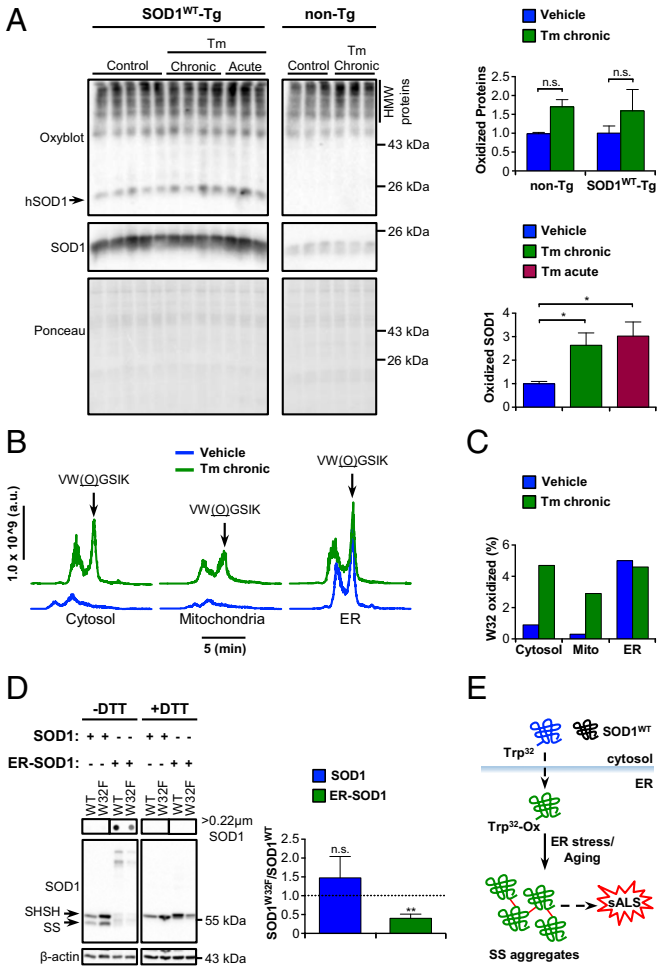

Fig. 4. Posttranslational modification and aggregation of SOD1^{WT} in the ER. (*A*) Western blot analysis of carbonylated (oxidized) proteins in total extracts of SOD1^{WT}-Tg mice and non-Tg littermates submitted to tunicamycin treatments as indicated. The arrow points to oxidized SOD1^{WT}. Ponceau S staining was employed as loading control. Statistical analysis was performed using two-way ANOVA (*Upper*) or one-way ANOVA (*Lower*) with Tukey's multiple comparison test. Mean ± SE is shown; *P* values are as follows: n.s., $P > 0.05$; $*P \leq 0.05$. $n = 3$ to 5 per group. (*B* and *C*) Mass spectrometry analysis of posttranslational modifications of SOD1^{WT} isolated from spinal cord subcellular fractions of SOD1^{WT}-Tg mice submitted to chronic Tm treatment. Seven animals were pooled in each sample. (*B*) Liquid chromatograms of a double-charged precursor ion with $m/z = 353.20$. Arrows indicate the peptide with oxidized tryptophan 32 [VW(O)GSIK]. Chromatograms were aligned to facilitate visualization. (*C*) Quantification of the percentage of SOD1 containing oxidized W32. (*D*) NSC-34 cells were transiently transfected for overexpression of SOD1^{WT}-EGFP, SOD1^{W32F}-EGFP, ER-SOD1^{WT}-EGFP, or ER-SOD1^{W32F}-EGFP. Filter-trap and Western blot analyses under nonreducing (–DTT) and reducing (+DTT) conditions were performed 48 h after transfection. Arrows indicate reduced (SHSH) or oxidized (SS) SOD1^{WT} monomer. The graph shows the ratio of SOD1^{W32F} to SOD1^{WT} total protein levels. Statistical analysis was performed using Student's *t* test. Mean ± SE is shown; *P* values are as follows: n.s., $P > 0.05$; $**P \leq 0.01$. $n = 3$. (*E*) Schematic model for SOD1^{WT} aggregation in the ER. Dashed arrows indicate unidentified pathways.

soluble species (9, 32), yielding a diffuse staining pattern in sALS tissue (8, 9). Some studies have challenged the participation of SOD1^{WT} in sALS pathogenesis based on the lack of staining with conformationally sensitive antibodies (18, 32, 33). These reports showed that antigen-retrieval treatments can enhance staining of SOD1^{WT} and mutant SOD1 with diverse conformation-specific antibodies and detect protein inclusions in SOD1-positive fALS, but not sALS, cases (18, 32, 33). However, the staining pattern of mutant SOD1 in patient samples may actually reflect the high protein concentration in SOD1-positive inclusions and should not be used as a main argument to rule out SOD1^{WT} involvement in sALS. As an alternative approach, immunoprecipitation with conformationally sensitive antibodies has been used to detect misfolded SOD1^{WT} in frozen sALS tissue, resulting in divergent conclusions (10, 18). Although misfolded and oxidized SOD1^{WT} species have been shown to have adverse consequences to motoneurons (9, 10, 28), their detection in sALS is not ubiquitous and may depend on the antibody employed and patient cohort (8–10, 17, 18). Moreover, there is scarce knowledge about the mechanisms contributing to SOD1^{WT} misfolding and aggregation in vivo.

To tackle this question, we employed transgenic mice overexpressing human SOD1^{WT} to investigate whether normal aging and ER stress could contribute to SOD1^{WT} aggregation and the appearance of disease features. Remarkably, we discovered that disulfide–cross-linked SOD1^{WT} aggregates accumulate in middle-aged mice whereas other aberrant SOD1^{WT} forms are detected only late, in aged animals. Subcellular fractionation of spinal cord showed that microsomes exclusively accumulate disulfide-dependent SOD1^{WT} aggregates with aging. Moreover, the ER-targeted overexpression of SOD1^{WT} greatly favored protein aggregation through disulfide cross-links, which is significantly inhibited by enforcing PDI expression. Together, these data indicate that ER localization favors SOD1^{WT} aggregation due to altered redox folding. ER stress is an early and transversal pathogenic mechanism in ALS that may explain the differential neuronal vulnerability (23). In this context, we investigated the relationship between ER stress and SOD1^{WT} misfolding and aggregation in vivo. Here we identified the selective accumulation of HMW disulfide–cross-linked SOD1^{WT} aggregates as the molecular signature of chronic ER stress in vivo. Thus, we reason that normal aging and chronic ER stress possibly share molecular mechanisms causing SOD1^{WT} aggregation in the ER (Fig. 4*E*). Similarly, we recently reported the presence of HMW disulfide–cross-linked aggregates of mutant TDP-43 in transgenic mice (34).

The identification of SOD1^{WT} aggregates in mice undergoing ER stress may be of relevance for sALS, since we were able to detect a significant increase in the levels of these SOD1^{WT} species in a subset of sALS patients (4 positive/7 total) accompanied by altered levels of ER chaperones. Moreover, disulfide–cross-linked SOD1 aggregation is a salient feature of mutant SOD1 ALS mouse models that sharply increases with disease progression and severity (35–38). It remains to be determined if the occurrence of SOD1^{WT} misfolding triggered by ER stress enhances its spreading through the nervous system. Although the induction of ER stress in human SOD1^{WT} transgenic mice was not sufficient to trigger motoneuron loss in the time frame of the study, it caused a selective activation of astrocytes in these animals. Since astrocyte activation is a relevant factor contributing to ALS pathogenesis (1), our observations suggest that the interplay between ER stress and SOD1^{WT} aggregation may influence cell-nonautonomous pathogenic mechanisms.

The analysis of posttranslational modifications of SOD1^{WT} identified microsomal SOD1^{WT} containing oxidized W32, indicating that the ER environment contributes to generation of aggregation-prone forms of the protein. The pattern of W32-oxidized SOD1^{WT} distribution under ER stress reveals a complex scenario where SOD1^{WT} may leak from the ER into mitochondria and cytosol, likely propagating protein aggregation in the intracellular milieu. This hypothesis remains to be explored. However, ER permeabilization under ER stress has been described to mediate the release of intraluminal components into the cytosol (39). Our results suggest that SOD1 trafficking through the ER is susceptible to W32 oxidation, facilitating disulfide-dependent protein aggregation (Fig. 4*E*). Importantly, W32 oxidation has also been associated with mutant SOD1 toxicity (40). Overall, this study uncovered an unexpected link

between ER stress and SOD1^{WT} aggregation with implications for understanding sALS pathogenesis.

Materials and Methods

Human Samples. Frozen postmortem spinal cord tissue from sALS patients and control subjects was obtained from the Alzheimer Disease Research Center at Massachusetts General Hospital and the R.H.B. laboratory at the Department of Neurology of University of Massachusetts Medical School under an approved institutional review board protocol (FWA 00004009). Written informed consent was obtained from all donors before tissue collection. The analysis of the human samples was also authorized by the Ethics Committee of the Faculty of Medicine of the University of Chile.

Animals. The experimental procedures using animals were approved by the Institutional Review Board for Animal Care of the Faculty of Medicine of the University of Chile (protocol 0503). The human SOD1^{WT}-Tg (transgenic) and SOD1^{G93A}-Tg mouse lines were purchased from The Jackson Laboratory and maintained on a C57BL/6 background. Details are given in *SI Appendix, Materials and Methods*.

ACKNOWLEDGMENTS. We thank Isabel Constantino and Diane McKenna-Yasek for their procurement of human tissue samples. We also thank John Leszyk and Scott Shaffer of the Proteomics and Mass Spectrometry Facility, University of Massachusetts Medical School. This work was funded by FONDAP (Fondo de Financiamiento de Centros de Investigación en Áreas Prioritarias) program 15150012, Millennium Institute P09-015-F, FONDECYT (Fondo Nacional de Desarrollo Científico y Tecnológico) 1180186, ALS Therapy Alliance 2014-F-059, Muscular Dystrophy Association 382453, Department of Defense ALS Research Program Award 81XWH-16-1-0112 (to C.H.), FONDECYT 3130351 and 11150579 (to D.B.M.), FONDECYT 3110067 and 1150743 (to U.W.), and National Institutes of Health Grant R01NS067206 (to D.A.B.). R.H.B. receives support from the National Institute of Neurological Disorders and Stroke (NINDS), the ALS Association, ALS Finding a Cure, ALS ONE, the Angel Fund for ALS Research, the Celluci Endowment for ALS Research, and Project ALS.

1. Taylor JP, Brown RH, Jr, Cleveland DW (2016) Decoding ALS: From genes to mechanism. *Nature* 539:197–206.
2. Turner MR, et al. (2013) Controversies and priorities in amyotrophic lateral sclerosis. *Lancet Neurol* 12:310–322.
3. Al-Chalabi A, Hardiman O (2013) The epidemiology of ALS: A conspiracy of genes, environment and time. *Nat Rev Neurol* 9:617–628.
4. Valentine JS, Doucette PA, Zittin Potter S (2005) Copper-zinc superoxide dismutase and amyotrophic lateral sclerosis. *Annu Rev Biochem* 74:563–593.
5. Sheng Y, Chattopadhyay M, Whitelegge J, Valentine JS (2012) SOD1 aggregation and ALS: Role of metallation states and disulfide status. *Curr Top Med Chem* 12: 2560–2572.
6. Peters OM, Ghasemi M, Brown RH, Jr (2015) Emerging mechanisms of molecular pathology in ALS. *J Clin Invest* 125:2548.
7. Philips T, Robberecht W (2011) Neuroinflammation in amyotrophic lateral sclerosis: Role of glial activation in motor neuron disease. *Lancet Neurol* 10:253–263.
8. Forsberg K, et al. (2010) Novel antibodies reveal inclusions containing non-native SOD1 in sporadic ALS patients. *PLoS One* 5:e11552.
9. Bosco DA, et al. (2010) Wild-type and mutant SOD1 share an aberrant conformation and a common pathogenic pathway in ALS. *Nat Neurosci* 13:1396–1403.
10. Grad LI, et al. (2014) Intercellular propagated misfolding of wild-type Cu/Zn superoxide dismutase occurs via exosome-dependent and -independent mechanisms. *Proc Natl Acad Sci USA* 111:3620–3625.
11. Fujisawa T, et al. (2012) A novel monoclonal antibody reveals a conformational alteration shared by amyotrophic lateral sclerosis-linked SOD1 mutants. *Ann Neurol* 72: 739–749.
12. Rotunno MS, Bosco DA (2013) An emerging role for misfolded wild-type SOD1 in sporadic ALS pathogenesis. *Front Cell Neurosci* 7:253.
13. Rakhit R, et al. (2002) Oxidation-induced misfolding and aggregation of superoxide dismutase and its implications for amyotrophic lateral sclerosis. *J Biol Chem* 277: 47551–47556.
14. Medinas DB, Gozzo FC, Santos LFA, Iglesias AH, Augusto O (2010) A ditryptophan cross-link is responsible for the covalent dimerization of human superoxide dismutase 1 during its bicarbonate-dependent peroxidase activity. *Free Radic Biol Med* 49: 1046–1053.
15. Jaarsma D, et al. (2000) Human Cu/Zn superoxide dismutase (SOD1) overexpression in mice causes mitochondrial vacuolization, axonal degeneration, and premature motoneuron death and accelerates motoneuron disease in mice expressing a familial amyotrophic lateral sclerosis mutant SOD1. *Neurobiol Dis* 7:623–643.
16. Graffmo KS, et al. (2013) Expression of wild-type human superoxide dismutase-1 in mice causes amyotrophic lateral sclerosis. *Hum Mol Genet* 22:51–60.
17. Liu H-N, et al. (2009) Lack of evidence of monomer/misfolded superoxide dismutase-1 in sporadic amyotrophic lateral sclerosis. *Ann Neurol* 66:75–80.
18. Da Cruz S, et al. (2017) Misfolded SOD1 is not a primary component of sporadic ALS. *Acta Neuropathol* 134:97–111.
19. Medinas DB, Valenzuela V, Hetz C (2017) Proteostasis disturbance in amyotrophic lateral sclerosis. *Hum Mol Genet* 26:R91–R104.
20. Hetz C, Saxena S (2017) ER stress and the unfolded protein response in neurodegeneration. *Nat Rev Neurol* 13:477–491.
21. Walter P, Ron D (2011) The unfolded protein response: From stress pathway to homeostatic regulation. *Science* 334:1081–1086.
22. Hetz C, Papa F (2018) The unfolded protein response and cell fate control. *Mol Cell* 69:169–181.
23. Rozas P, Bargsted L, Martínez F, Hetz C, Medinas DB (2017) The ER proteostasis network in ALS: Determining the differential motoneuron vulnerability. *Neurosci Lett* 636:9–15.
24. Saxena S, Cabuy E, Caroni P (2009) A role for motoneuron subtype-selective ER stress in disease manifestations of FALS mice. *Nat Neurosci* 12:627–636.
25. Kikuchi H, et al. (2006) Spinal cord endoplasmic reticulum stress associated with a microsomal accumulation of mutant superoxide dismutase-1 in an ALS model. *Proc Natl Acad Sci USA* 103:6025–6030.
26. Turner BJ, et al. (2005) Impaired extracellular secretion of mutant superoxide dismutase 1 associates with neurotoxicity in familial amyotrophic lateral sclerosis. *J Neurosci* 25:108–117.
27. Kaushik S, Cuervo AM (2015) Proteostasis and aging. *Nat Med* 21:1406–1415.
28. Guareschi S, et al. (2012) An over-oxidized form of superoxide dismutase found in sporadic amyotrophic lateral sclerosis with bulbar onset shares a toxic mechanism with mutant SOD1. *Proc Natl Acad Sci USA* 109:5074–5079.
29. Urushitani M, Ezzi SA, Julien J-P (2007) Therapeutic effects of immunization with mutant superoxide dismutase in mice models of amyotrophic lateral sclerosis. *Proc Natl Acad Sci USA* 104:2495–2500.
30. Hatahet F, Ruddock LW (2009) Protein disulfide isomerase: A critical evaluation of its function in disulfide bond formation. *Antioxid Redox Signal* 11:2807–2850, and erratum (2010) 12:322.
31. Schmitt ND, Agar JN (2017) Parsing disease-relevant protein modifications from epiphenomena: Perspective on the structural basis of SOD1-mediated ALS. *J Mass Spectrom* 52:480–491.
32. Brotherton TE, et al. (2012) Localization of a toxic form of superoxide dismutase 1 protein to pathologically affected tissues in familial ALS. *Proc Natl Acad Sci USA* 109: 5505–5510.
33. Ayers JI, et al. (2014) Conformational specificity of the C4F6 SOD1 antibody; low frequency of reactivity in sporadic ALS cases. *Acta Neuropathol Commun* 2:55.
34. Bargsted L, et al. (2017) Disulfide cross-linked multimers of TDP-43 and spinal motoneuron loss in a TDP-43^{A315T} ALS/FTD mouse model. *Sci Rep* 7:14266.
35. Furukawa Y, Fu R, Deng H-X, Siddique T, O'Halloran TV (2006) Disulfide cross-linked protein represents a significant fraction of ALS-associated Cu, Zn-superoxide dismutase aggregates in spinal cords of model mice. *Proc Natl Acad Sci USA* 103: 7148–7153.
36. Jonsson PA, et al. (2006) Disulphide-reduced superoxide dismutase-1 in CNS of transgenic amyotrophic lateral sclerosis models. *Brain* 129:451–464.
37. Wang J, Xu G, Borchelt DR (2006) Mapping superoxide dismutase 1 domains of nonnative interaction: Roles of intra- and intermolecular disulfide bonding in aggregation. *J Neurochem* 96:1277–1288.
38. Deng H-X, et al. (2006) Conversion to the amyotrophic lateral sclerosis phenotype is associated with intermolecular linked insoluble aggregates of SOD1 in mitochondria. *Proc Natl Acad Sci USA* 103:7142–7147.
39. Pihán P, Carreras-Sureda A, Hetz C (2017) BCL-2 family: Integrating stress responses at the ER to control cell demise. *Cell Death Differ* 24:1478–1487.
40. Taylor DM, et al. (2007) Tryptophan 32 potentiates aggregation and cytotoxicity of a copper/zinc superoxide dismutase mutant associated with familial amyotrophic lateral sclerosis. *J Biol Chem* 282:16329–16335.